Physics. — *The intensities of direct and scattered X-radiation in a horizontal water sheet exposed to a cylindriform beam of soft vertical X-rays.* By R. H. DE WAARD. (X-ray department of the Medical University Clinic, Utrecht.) (Communicated by Prof. H. R. KRUYT.)

(Communicated at the meeting of May 31, 1947.)

1. *Introduction.*

Various illnesses are, nowadays, treated with X-rays. In a simple treatment some definite part of the skin is exposed to a beam of X-radiation, and it is important to know what, in such a case, the distribution of direct and scattered radiation will be in the patients body.

Distributions of this sort have often been investigated by measurements on waterphantoms. In this paper it will be shown that in several cases these distributions can also be approximated theoretically.

2. *Statement of the problem and its mathematical expression by an integral equation.*

The theoretical developments to be given in this paper refer to the arrangement represented in fig. 1. On the surface of a horizontal water

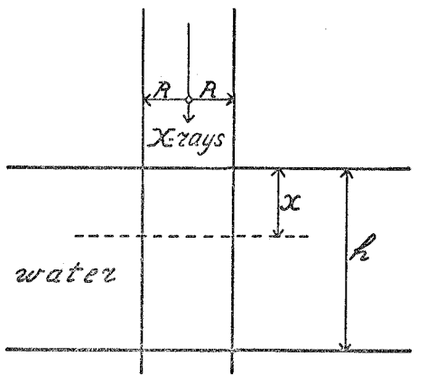

Fig. 1. Cylindriform beam of vertical X-rays falling on a horizontal watersheet of thickness h. R: radius of a horizontal cross-section of the beam.

sheet falls a cylindriform beam of vertical X-rays having all the same wavelength λ, the thickness of the sheet being denoted by h and the radius of the beam by R.

Now the intensities of direct and scattered X-radiation in the water sheet can be approximately calculated by a method given by the author in a preceding paper [1]). It was assumed in this paper that in any given level

[1]) The intensity of scattered X-radiation in medical radiography. Proc. Kon. Ned. Akad. v. Wetensch.., Amsterdam, **49**, 955—966 and 1016—1024 (1946).

the intensity of scattered radiation is constant throughout the original beam and zero beyond it. In the present paper we will denote by S_x and D_x the intensities of scattered and direct radiation in a level at distance x under the water surface; D_0 is then the intensity of the incident radiation and we have

$$D_x = D_0\, e^{-\mu x} \quad . \quad . \quad . \quad . \quad . \quad . \quad . \quad . \quad . \quad (1)$$

where

$$\mu = 2.5\,\lambda^3 + 0.18 \quad . \quad . \quad . \quad . \quad . \quad . \quad . \quad . \quad (2)$$

is the coefficient of enfeeblement of the X-radiation in question when propagating in water. When, moreover, we assume that the distribution of scattered radiation over various directions is given by J. J. THOMSON's well-known formula [2]) S_x will satisfy the integral equation

$$\left.\begin{aligned} S_x = &\int_0^x \{D_0\, e^{-\mu y} + S_y\}\, \Phi_{\mu R}\{\mu(x-y)\}\, dy + \\ &+ \int_x^h \{D_0\, e^{-\mu y} + S_y\}\, \Phi_{\mu R}\{\mu(y-x)\}\, dy \end{aligned}\right\} \quad . \quad . \quad . \quad (3)$$

where

$$\Phi_{\mu R}(u) = \tfrac{3}{8} \times 0.18 \left[\left(1 + \frac{u^2}{2}\right) \int_0^\infty \frac{e^{-z}}{z}\, dz + \frac{u^2}{2}\, \frac{1-z}{z}\, e^{-z} \right]_{z=\sqrt{u^2+(\mu R)^2}}^{z=u}.$$

This integral equation is not essentially different from the one treated in the preceding paper mentioned, and an approximate solution can be obtained in very much the same way.

3. *Approximate solution of the integral equation.*

It was found in the paper mentioned that the function $\Phi_{\mu R}(u)$ can be conveniently approximated by an expression of the form

$$\Psi_{\mu R}(u) = k_1\, e^{-\gamma_1 u} + k_2\, e^{-\gamma_2 u} \quad . \quad . \quad . \quad . \quad . \quad . \quad . \quad (4)$$

where $k_1 = 0.200$ and $\gamma_1 = 10$ whilst the constants k_2 and γ_2 are different for different values of μR and can be derived from the graphs of fig. 2. Now, when in the integral equation (3) we replace $\Phi_{\mu R}(u)$ by the expression for $\Psi_{\mu R}(u)$ we arrive at an integral equation which can be solved by elementary methods. The solution is

$$S_x = D_0 \left(\frac{m}{1-m}\, e^{-\mu x} + g_{11}\, e^{-\xi x} + g_{12}\, e^{\xi x} + g_{21}\, e^{-\eta x} + g_{22}\, e^{\eta x} \right) . \quad (5)$$

where the constants m, ξ, η are given by the formulae

$$m = \frac{2k_1(\mu\gamma_1)}{(\mu\gamma_1)^2 - \mu^2} + \frac{2k_2(\mu\gamma_2)}{(\mu\gamma_2)^2 - \mu^2} \quad . \quad . \quad . \quad . \quad . \quad . \quad (6)$$

[2]) See M. et L. DE BROGLIE, Introduction à la Physique des Rayons X et Gamma, Paris 1928, pp. 131—138.

and

$$\left.\begin{aligned} \xi &= \sqrt{\tfrac{1}{2}p - \sqrt{\tfrac{1}{4}p^2 - q}} \qquad \eta = \sqrt{\tfrac{1}{2}p + \sqrt{\tfrac{1}{4}p^2 - q}} \\ \text{with} \quad p &= (\mu\gamma_1)^2 + (\mu\gamma_2)^2 - 2k_1(\mu\gamma_1) - 2k_2(\mu\gamma_2) \\ \text{and} \quad q &= (\mu\gamma_1)^2(\mu\gamma_2)^2\left(1 - \frac{2k_1}{\mu\gamma_1} - \frac{2k_2}{\mu\gamma_2}\right) \end{aligned}\right\} \quad . \; . \; (7)$$

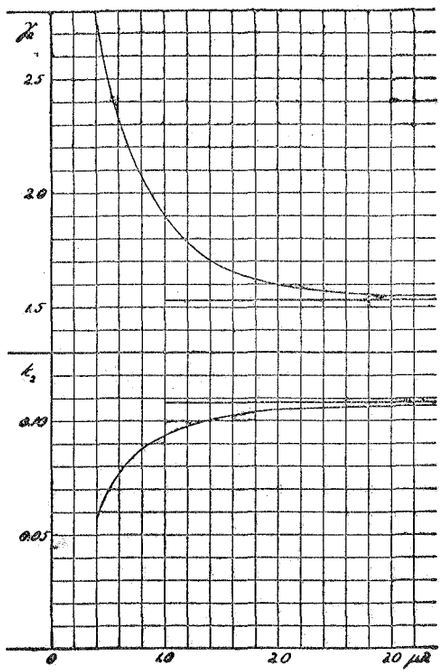

Fig. 2. Graphs showing the dependence of k_2 and γ_2 on μR.

whilst the values of the quantities g can be derived from the equations

$$\left.\begin{aligned} &\frac{1}{(1-m)e_1} + \frac{g_{11}}{a_1} + \frac{g_{12}}{a_3} + \frac{g_{21}}{b_1} + \frac{g_{22}}{b_3} = 0 \\ &\frac{1}{(1-m)e_2} + \frac{g_{11}}{a_2} + \frac{g_{12}}{a_4} + \frac{g_{21}}{b_2} + \frac{g_{22}}{b_4} = 0 \\ &\frac{e^{-\mu h}}{(1-m)e_3} + \frac{g_{11}e^{-\xi h}}{a_3} + \frac{g_{12}e^{\xi h}}{a_1} + \frac{g_{21}e^{-\eta h}}{b_3} + \frac{g_{22}e^{\eta h}}{b_1} = 0 \\ &\frac{e^{-\mu h}}{(1-m)e_4} + \frac{g_{11}e^{-\xi h}}{a_4} + \frac{g_{12}e^{\xi h}}{a_2} + \frac{g_{21}e^{-\eta h}}{b_4} + \frac{g_{22}e^{\eta h}}{b_2} = 0 \end{aligned}\right\} \quad . \; (8)$$

where

$$\left.\begin{aligned} e_1 &= \mu\gamma_1 - \mu & a_1 &= \mu\gamma_1 - \xi & b_1 &= \mu\gamma_1 - \eta \\ e_2 &= \mu\gamma_2 - \mu & a_2 &= \mu\gamma_2 - \xi & b_2 &= \mu\gamma_2 - \eta \\ e_3 &= \mu\gamma_1 + \mu & a_3 &= \mu\gamma_1 + \xi & b_3 &= \mu\gamma_1 + \eta \\ e_4 &= \mu\gamma_2 + \mu & a_4 &= \mu\gamma_2 + \xi & b_4 &= \mu\gamma_2 + \eta \end{aligned}\right\} . \quad (9)$$

The total intensity J_x in the level at distance x under the water surface is then

$$J_x = S_x + D_x = D_0\left(\frac{e^{-\mu x}}{1-m} + g_{11}e^{-\xi x} + g_{12}e^{\xi x} + g_{21}e^{-\eta x} + g_{22}e^{\eta x}\right) \quad (10)$$

4. *Discussion of the case of thick watersheets.*

The most important case is that where the watersheet is rather thick. In this case the necessary calculations are comparatively simple. We can obtain the total intensity J_x in levels at some distance from the bottom by putting $h = \infty$ in the equations (8) and substituting the resulting values of the quantities g in (10). Now by doing so we find from the last two equations (8) that

$$g_{12} = g_{22} = 0;$$

the first two equations then give

$$g_{11} = \frac{-\frac{a_2}{e_2}\left(1 - \frac{e_2}{e_1}\frac{b_1}{b_2}\right)}{(1-m)\left(1 - \frac{a_2}{a_1}\frac{b_1}{b_2}\right)} \quad \text{and} \quad g_{21} = \frac{-\frac{b_1}{e_1} + \frac{b_1}{e_1}\frac{a_2}{a_1}}{(1-m)\left(1 - \frac{a_2}{a_1}\frac{b_1}{b_2}\right)}$$

and so, as $\frac{a_2}{a_1} \times \frac{b_1}{b_2}$ and $\frac{e_2}{e_1} \times \frac{b_1}{b_2}$ appear to be small quantities, the formula for J_x may be written

$$J_x = D_0\left(\frac{e^{-\mu x}}{1-m} + P\,e^{-\xi x} + Q\,e^{-\eta x}\right) \quad . \; . \; . \; . \quad (11)$$

where

$$\left.\begin{aligned} P &= \frac{-1}{1-m} \cdot \frac{a_2}{e_2}\left\{1 - \frac{b_1}{b_2}\left(\frac{e_2}{e_1} - \frac{a_2}{a_1}\right)\right\} \\ \text{and} \quad Q &= \frac{-1}{1-m}\left(\frac{b_1}{e_1} - \frac{b_1}{e_2}\frac{a_2}{a_1}\right)\left(1 + \frac{a_2}{a_1}\frac{b_1}{b_2}\right) \end{aligned}\right\} \quad . \; . \; . \; . \; . \quad (12)$$

This formula will now be applied in some special cases.

Case Ia. $\mu = 0.30$, $R = 10$ cm.

Formula (2) gives the corresponding wavelength λ to 0.363 Å. From the curves of fig. 2 we can derive $k_2 = 0.1066$, $\gamma_2 = 1.55$ whilst $k_1 = 0.200$, $\gamma_1 = 10.0$. Substituting these numbers in (6) and (7) and then applying (9) and (11) we find

$$J_x = D_0\,(15.533\,e^{-0.3x} - 14.095\,e^{-0.315x} - 0.103\,e^{-2.80x}). \quad . \quad (13)$$

The relation between J_x and x given by this formula is graphically represented by the upper curve of fig. 3. In this curve is slightly indicated that

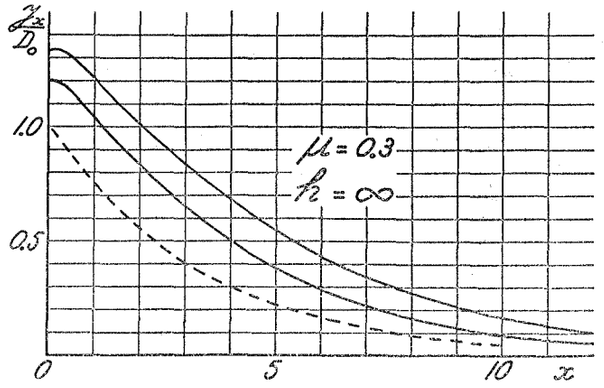

Fig. 3. Full curves: calculated values of $\frac{J_x}{D_0}$ at various depths in the watersheet.
Upper curve: $\mu = 0.3$ ($\lambda = 0.363$ Å), $R = 10$ cm.
Lower curve: $\mu = 0.3$ ($\lambda = 0.363$ Å), $R = 2.5$ cm.
Dotted curve: relative values $\frac{D_x}{D_0}$ of the intensity of direct radiation.

the total X-ray intensity J_x has a maximum at some distance under the water surface. A tendency to the formation of such a maximum is also found in the lower full curve, but here is not actually present. The latter curve refers to

Case I*b*. $\mu = 0.30$, $R = 2.5$ cm.

Here we have $k_2 = 0.085$, $\gamma_2 = 2.12$ (see fig. 2), and the resulting formula for J_x is

$$J_x = D_0 (1.917\, e^{-0.3x} - 0.614\, e^{-0.528x} - 0.094\, e^{-2.80x}). \quad . \quad (14)$$

The dotted curve in fig. 3 gives the contribution to J_x which is due to direct radiation, and so the figure clearly shows the importance of the process of scattering.

A comparison of the full curves shows us the influence of the size of the incident beam. The influence of the wavelength becomes apparent when we compare these curves with the full curve of fig. 4 which corresponds to either of the following two cases:

Case II*a*. $\mu = 0.60$, $R = 10$ cm.

$$\lambda = 0.552 \text{ Å} \qquad k_2 = 0.108 \qquad \gamma_2 = 1.53$$
$$J_x = D_0 (1.916\, e^{-0.6x} - 0.750\, e^{-0.794x} - 0.042\, e^{-5.80x}). \quad . \quad (15)$$

Case II*b*. $\mu = 0.60$, $R = 2.5$ cm.

$$\lambda = 0.552 \text{ Å} \qquad k_2 = 0.101 \qquad \gamma_2 = 1.68$$
$$J_x = D_0 (1.607\, e^{-0.6x} - 0.453\, e^{-0.894x} - 0.042\, e^{-5.80x}). \quad . \quad (16)$$

In these cases the influence of scattering is not so important as in the cases I*a* and I*b*.

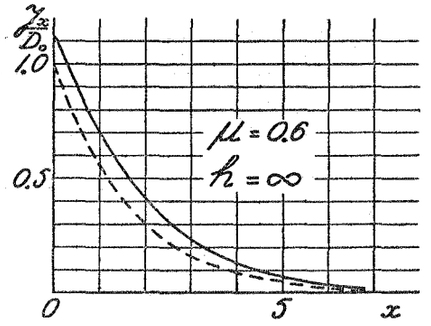

Fig. 4. Full curve: calculated relation between $\frac{J_x}{D_0}$ and x for $\mu = 0.6$ ($\lambda = 0.552$ Å), $R = 2.5$ cm.
This curve is not sensibly different from that for $\mu = 0.6$ ($\lambda = 0.552$ Å), $R = 10$ cm.
Dotted curve: relation between $\frac{D_x}{D_0}$ and x.

5. *Watersheets of moderate thickness.*

The formulae (11) and (12) obtained in the preceding section for the total X-ray intensity J_x refer to the limit case of infinitely thick watersheets. In the present section we will derive formulae applying to the case of watersheets of moderate thickness.

It is obvious that we can obtain general formulae for the coefficients g figuring in (10) by solving the set of linear equations (8). We have for instance:

$$g_{11} = \frac{\begin{vmatrix} \frac{1}{a_3} & \frac{1}{b_1} \\ \frac{1}{a_4} & \frac{1}{b_2} \end{vmatrix} \begin{vmatrix} \frac{1}{e_3} & \frac{1}{b_1} \\ \frac{1}{e_4} & \frac{1}{b_2} \end{vmatrix} e^{(-\mu+\eta)h} - \begin{vmatrix} \frac{1}{e_1} & \frac{1}{b_1} \\ \frac{1}{e_2} & \frac{1}{b_2} \end{vmatrix} \begin{vmatrix} \frac{1}{a_1} & \frac{1}{b_1} \\ \frac{1}{a_2} & \frac{1}{b_2} \end{vmatrix} e^{(\xi+\eta)h} + 4 \text{ other terms}}{(1-m)\left\{ 2 \begin{vmatrix} \frac{1}{a_1} & \frac{1}{a_3} \\ \frac{1}{a_2} & \frac{1}{a_4} \end{vmatrix} \begin{vmatrix} \frac{1}{b_3} & \frac{1}{b_1} \\ \frac{1}{b_4} & \frac{1}{b_2} \end{vmatrix} + \begin{vmatrix} \frac{1}{a_3} & \frac{1}{b_1} \\ \frac{1}{a_4} & \frac{1}{b_2} \end{vmatrix}^2 e^{(-\xi+\eta)h} + 3 \text{ other terms} \right\}}$$

We will now confine ourselves to the consideration of cases where the watersheet in question is more than 4 cm thick. Numerical calculations show that several of the terms figuring in the expression for g_{11} may then be neglected and that the expression can be reduced to

$$g_{11} = \frac{\frac{a_2}{a_4}\frac{a_2}{e_4} e^{(-\mu-\xi)h} - \frac{a_2}{e_2}\left\{1 - \frac{b_1}{b_2}\left(\frac{e_2}{e_1} - \frac{a_2}{a_1}\right)\right\}}{(1-m)\left\{1 - \left(\frac{a_2}{a_4}\right)^2 e^{-2\xi h}\right\}}$$

In a similar way can be obtained the following expressions for the other quantities g:

$$g_{12}=\frac{\left(-\frac{a_2}{e_4}+\frac{a_2}{b_2}\frac{b_1}{e_3}\right)\left(1+\frac{a_2}{a_1}\frac{b_1}{b_2}\right)e^{-\mu h}+\frac{a_2}{e_2}\frac{a_2}{a_4}\left\{1+\frac{b_1}{b_2}\left(2\frac{a_2}{a_1}-\frac{e_2}{e_1}-\frac{a_4}{a_3}\right)\right\}e^{-\xi h}}{(1-m)\left\{1-\left(\frac{a_2}{a_4}\right)^2 e^{-2\xi h}\right\}}e^{-\xi h}$$

$$g_{21}=\frac{-\frac{b_1}{e_1}+\frac{a_2}{a_1}\frac{b_1}{e_2}-\frac{a_2}{a_4}\frac{b_1}{a_3}\frac{a_2}{e_2}\left(1-\frac{a_3}{a_4}\frac{e_2}{e_1}\right)e^{-2\xi h}}{(1-m)\left\{1-\left(\frac{a_2}{a_4}\right)^2 e^{-2\xi h}\right\}}$$

$$g_{22}=\frac{\left(-\frac{b_1}{e_3}+\frac{a_2}{a_1}\frac{b_1}{e_4}\right)\left(1+\frac{a_2}{a_1}\frac{b_1}{b_2}\right)e^{-\mu h}+\frac{a_2}{e_2}\left(\frac{b_1}{a_3}-\frac{b_1}{a_4}\frac{a_2}{a_1}\right)\left\{1-\frac{b_1}{b_2}\left(\frac{e_2}{e_1}-2\frac{a_2}{a_1}\right)\right\}e^{-\xi h}}{(1-m)\left\{1-\left(\frac{a_2}{a_4}\right)^2 e^{-2\xi h}\right\}}e^{-\eta h}$$

We will now apply these formulae to some cases where $h=5$ cm, 10 cm and 20 cm, and compare the results with those obtained in section 4 for watersheets of infinite thickness.

Case Ia. $\mu=0.30$, $R=10$ cm.

The coefficients figuring in the right hand member of (10) are given by the formulae

$$\xi=0.315 \qquad \eta=2.80 \qquad \frac{1}{1-m}=15.533$$

$$g_{11}=\frac{0.567\,e^{-0.615h}-14.102}{1-0.036\,e^{-0.63h}}$$

$$g_{12}=\frac{-3.042\,e^{-0.3h}+2.710\,e^{-0.315h}}{1-0.036\,e^{-0.63h}}e^{-0.315h}$$

$$g_{21}=\frac{-0.103-0.122\,e^{-0.63h}}{1-0.036\,e^{-0.63h}}$$

$$g_{22}=\frac{-0.730\,e^{-0.3h}+0.663\,e^{-0.315h}}{1-0.036\,e^{-0.63h}}e^{-2.80h}$$

From the latter four of these formulae can be derived the values of the quantities g corresponding to different water-thicknesses h. The values for $h=\infty$, $h=20$ cm, $h=10$ cm and $h=5$ cm are given in Table Ia.

With the help of these values were obtained the J_x, x-curves corresponding to $h=\infty$, $h=10$ cm and $h=5$ cm which are shown in fig. 5;

TABLE Ia ($\mu=0.30$, $R=10$ cm).

h	∞	20 cm	10 cm	5 cm
g_{11}	-14.102	-14.102	-14.101	-14.076
$g_{12}e^{0.315h}$	0	-0.003	-0.035	-0.118
g_{21}	-0.103	-0.103	-0.103	-0.108
$g_{22}e^{2.976h}$	0	-0.001	-0.008	-0.026

a curve for $h=20$ cm has been omitted since it would not have differed much from that for $h=\infty$. Just as in figs. 3 and 4 the dotted curve gives the contribution to J_x which is due to direct radiation.

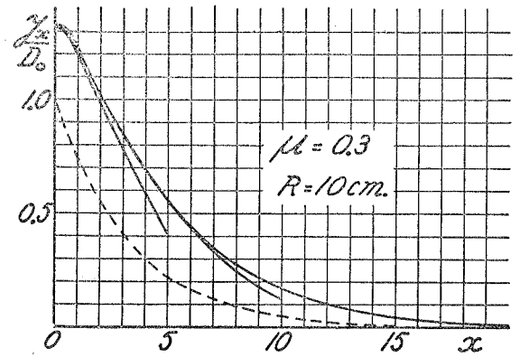

Fig. 5. Full curves: calculated relations between $\frac{J_x}{D_0}$ and x corresponding to the following cases:

Upper curve: $\mu=0.3$, $R=10$ cm, $h=\infty$
Middle curve: $\mu=0.3$, $R=10$ cm, $h=10$ cm
Lower curve: $\mu=0.3$, $R=10$ cm, $h=5$ cm

Dotted curve, relation between $\frac{D_x}{D_0}$ and x.

Case Ib. $\mu=0.30$, $R=2.5$ cm.

Here we have

$$\xi=0.528 \qquad \eta=2.80 \qquad \frac{1}{1-m}=1.917.$$

$$g_{11}=\frac{0.021\,e^{-0.828h}-0.619}{1-0.009\,e^{-1.056h}}$$

$$g_{12}=\frac{-0.225\,e^{-0.3h}+0.059\,e^{-0.528h}}{1-0.009\,e^{-1.056h}}e^{-0.528h}$$

$$g_{21}=\frac{-0.094-0.002\,e^{-1.056h}}{1-0.009\,e^{-1.056h}}$$

$$g_{22}=\frac{-0.100\,e^{-0.3h}+0.032\,e^{-0.528h}}{1-0.009\,e^{-1.056h}}e^{-2.80h}$$

If in the latter four of these formulae we substitute $h = \infty$, $h = 20$ cm, $h = 10$ cm and $h = 5$ cm we find the values of the quantities g which are given in Table I*b*.

TABLE I*b* ($\mu = 0.30$, $R = 2.5$ cm).

h	∞	20 cm	10 cm	5 cm
g_{11}	-0.614	-0.614	-0.614	-0.614
$g_{12}e^{0.528h}$	0	-0.001	-0.011	-0.046
g_{21}	-0.094	-0.094	-0.094	-0.094
$g_{22}e^{2.80h}$	0	0	-0.005	-0.020

The J_x, x-curves corresponding to $h = \infty$ and $h = 5$ cm are shown in fig. 6.

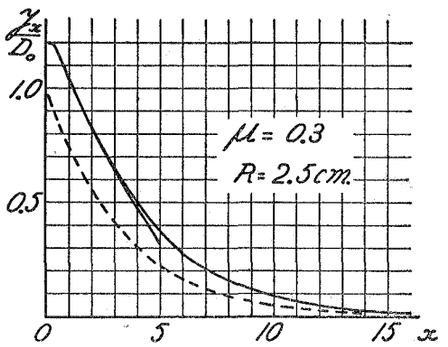

Fig. 6. Full curves: calculated relations between $\frac{J_x}{D_0}$ and x corresponding to the following cases:

Upper curve: $\mu = 0.3$, $R = 2.5$ cm, $h = \infty$
Lower curve: $\mu = 0.3$, $R = 2.5$ cm, $h = 5$ cm

Dotted curve: relation between $\frac{D_x}{D_0}$ and x.

As to the cases II*a* ($\mu = 0.60$, $R = 10$ cm) and II*b* ($\mu = 0.6$, $R = 2.5$ cm) it may be observed that the differences between the J_x, x-curves for $h = 20$ cm, $h = 10$ cm and $h = 5$ cm and those for $h = \infty$ given in fig. 4 are negligible.

6. *General discussion. Comparison with experimental data.*

The formulae for J_x obtained in this paper were derived from the integral equation (3) by a method of approximation which is perfectly justified. The integral equation itself, however, needs some discussion. One of the assumptions on which it is based is the validity of J. J. THOMSON's

classical theory of X-ray scattering. We know that this theory gives a reasonable approximation of facts when the wavelengths concerned are large with respect to the Compton-wavelength $\lambda_c = 0.024$ Å, but that it does not hold for smaller wavelengths (e.g. < 0.24 Å). When we have to deal with such smaller wavelengths we must account for a reduction of sideward and especially of backward scattering and, moreover, for the increase of wavelength known as the Compton-effect. Whilst these phenomena will only slightly reduce the influence of scattering in forward directions they may cause a considerable decrease of the influence of scattering in backward directions, and so we must expect that their neglection will, in the main, result in an overvaluation of the influence of backward scattering in the theory. To this divergence must be added an error due to another source. It was assumed in the deduction of the integral equation that scattered radiation of any order originating in some part of the watersheet has the same distribution over various directions as secondary radiation, and this results in the influence of both forward and backward scattering being exaggerated, particularly when the incident beam is large. In cases of large wavelengths and incident beams of moderate size, however, the final formulae for J_x may be fairly reliable, and the question arises whether we have at our disposal experimental data with which these formulae can be compared numerically. Now this appears to be actually the case. The curves of figs. 3 and 4 refer to incident beams of wavelengths $\lambda = 0.363$ Å and $\lambda = 0.552$ Å, and the formula

$$\mu = 37\,\lambda^3 + 0.38$$

for the coefficient of enfeeblement in aluminium gives the corresponding half value layers for this metal to 3.0 mm and 1.0 mm respectively. Now depth dose measurements on radiations with this sort of half value layers were carried out during the war by C. B. BRAESTRUP, and his results can be found in tables A—F at the end of the book "Physical Foundations of Radiology" by O. GLASSER, E. H. QUIMBY, L. S. TAYLOR and J. L. WEATHERWAX. However, the conditions of the experiments were rather different from those to which the calculations of this paper apply. The main differences are:

1. The calculations apply to cylindriform beams of parallel X-rays whereas the experiments were carried out with divergent beams, and

2. In the calculations the incident X-radiation is supposed to have one definite wavelength whereas in the experiments it formed a rather extensive continuous spectrum.

Now it is easy to see what effect these differences will have when we compare cases of equal half value layer and equal size of the exposed area of the water surface. Let us first consider the influence of the divergence of the incident beams which BRAESTRUP applied in his measurements. It is obvious that this divergence will result in a more rapid decrease of X-ray intensity on the way from the surface to the lower parts of the watersheet.

For the direct radiation the extra decrease is given by the inverse square law; in scattered radiation, however, a still stronger decrease of intensity must be expected on account of the fact that the mean distance of any part of the incident beam to the other parts increases with increasing cross-section.

As to the spectral composition of the incident radiation applied in the experiments it is clear that the more penetrating components will have greater importance according as we consider a lower level in the water-sheet. From this fact will result an increase of X-ray intensity in the lower levels and this increase may overcompensate the decrease due to the divergence of the incident beam.

There is, however, one point which is not affected by the discussed differences between theoretical and experimental conditions. This point is the X-ray intensity at the surface of the watersheet which is due to downward incident radiation and to upward backscatter. If, therefore, we express backscatter or total X-radiation at the water surface in terms of the incident radiation we should find close agreement between calculated and measured values. Now, in fact, the agreement between calculated and measured backscatter values is very satisfactory indeed. This is clearly shown by the curves of figs. 7 and 8 which refer to cases with half value

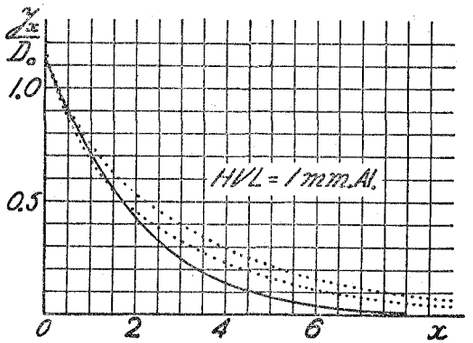

Fig. 7. Curves giving calculated and measured relations between $\frac{J_x}{D_0}$ and x for radiations with half-value layer of 1 mm Al.
Full curve (calculated): parallel X-rays of wavelength $\lambda = 0.552$ Å ($\mu = 0.6$), field of incidence 20 cm² or greater ($R = 2.5$ cm).
Dotted curves (measurements by C. B. BRAESTRUP): high tension 100 kV, inherent filter only, focus-surface distance 30 cm.
Upper dotted curve: field of incidence 100 cm² ($R = 11.3$ cm).
Lower dotted curve: field of incidence 25 cm² ($R = 5.6$ cm).

layers of 1 mm Al ($\mu = 0.6$ and $\lambda = 0.552$ Å in the calculations) and 4 mm Al ($\mu = 0.257$ and $\lambda = 0.313$ Å in the calculations). Corresponding to the lower levels of the watersheet the curves show discrepancies of the sort predicted in the above qualitative considerations, and so the formulae

obtained in this paper look like giving a good approximation of facts when the wavelength of the incident radiation is between 0.3 and 0.6 Å. It is therefore of interest that they give quantitative information on certain

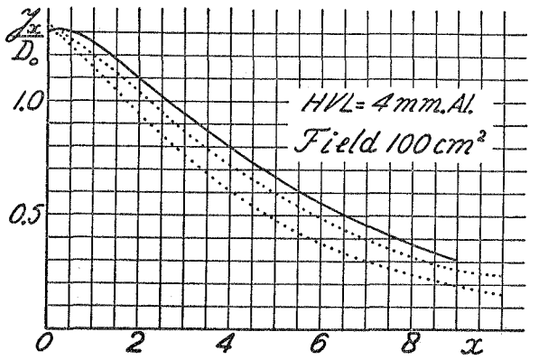

Fig. 8. Curves giving calculated and measured relations between $\frac{J_x}{D_0}$ and x for radiations with half-value-layer of 4 mm Al. and field of incidence of 100 cm² ($R = 5.64$ cm). Full curve (calculated): parallel X-rays of wavelength $\lambda = 0.363$ Å ($\mu = 0.3$). Dotted curves (measurements by C. B. BRAESTRUP): high tension 120 kV, filter 3 mm Al.
Upper dotted curve: focus surface distance 40 cm.
Lower dotted curve: focus surface distance 20 cm.

features which are not taken into account in current medical applications. In conclusion some of these features may be mentioned here:

a. The part of total X-radiation which is due to scattering is more important according as we have to do with thicker watersheets,

b. When compared with its general course in the central parts of the watersheet the intensity of total X-radiation shows a marked decrease not only towards the surface, but also towards the bottom of the sheet.

Summary.

A method is given by which can be approximately calculated the total intensity of X-radiation in various levels of a horizontal watersheet which is exposed to a cylindriform beam of soft vertical X-rays. The resulting formulae are in satisfactory agreement with the results of a series of measurements carried out during the war by C. B. BRAESTRUP. They give some quantitative information on certain features which are not taken into account in current medical applications.